Tutor/s
Dr. David Aguilà

Química Inorgànica i Orgànica
(secció Inorgànica)

Grau de Química

Treball Final de Grau

Design of spin-crossover heterometallic coordination compounds

Diseño de compuestos de coordinación heterometálicos con transición de espín

Celia Vilar Ayuso

June 2018

Universitat de Barcelona

B:KC Barcelona Knowledge Campus
Campus d'Excel·lència Internacional

I hadn't been aware that there were doors closed to me until I started knocking on them.

Gertrude Belle Elion

REPORT

CONTENTS

1. SUMMARY

This project has been fulfilled in the research Group of Magnetism and Functional Molecules (GMMF), at the University of Barcelona. The main purpose of this group is based on the synthesis and study of coordination compounds, which present different interesting physical properties. These fascinating compounds have many applications such as in quantum computing or nanotechnology.

In this project the design of new Spin Crossover (SCO) Fe(II)-based complexes able to produce heterometallic compounds, has been carried out. These Fe(II) complexes are formed by ligands based on derivatives of 2,6-bis(pyrazol-3-yl)pyridine (3-bpp) featuring external coordinating units, where other metals (transition metals or lanthanides) could be further coordinated *(Figure 1).* Moreover, they can exhibit one (homoleptic) or two different ligands (heteroleptic) to facilitate incorporating such additional ions. The derived heterometallic complexes could play an important role in quantum computing, with the Fe(II) SCO unit acting as a switch and the external metals as quantum bits.

To achieve this goal, it has been performed the synthesis and characterization of different organic ligands. Also, the potential coordination capabilities of one of them to produce Fe(II) complexes has been studied.

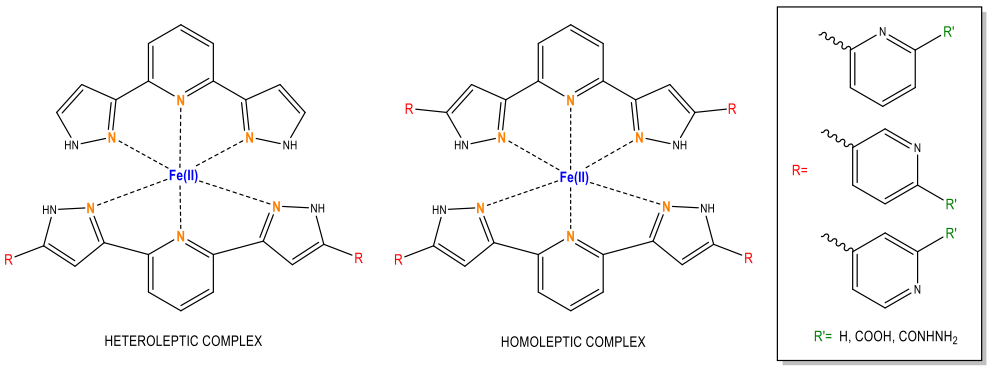

Figure 1. Heteroleptic and homoleptic complexes containing central coordination units and external coordination unities.

Keywords: Spin-crossover, coordination chemistry, Fe (II) complexes, organic ligands, metalloligands, quantum computing, molecular switch.

2. RESUM

Este proyecto se ha realizado en el Grupo de Magnetismo y Moléculas Funcionales (GMMF), en la Universidad de Barcelona. El objetivo principal de este grupo se basa en la síntesis y estudio de compuestos de coordinación que presentan propiedades físicas interesantes. Estos compuestos tienen diferentes aplicaciones como la computación cuántica o la nanotecnología.

En este proyecto se ha llevado a cabo el diseño de complejos de hierro (II) los cuales presentan la propiedad de transición de espín y pueden formar complejos heterometálicos. Estos complejos de Fe(II) están formados por ligandos basados en derivados de 2,6-bis(pirazol-3-il)piridina (3-bpp), con unidades de coordinación externas, donde otros metales (metales de transición o lantánidos) podrían coordinarse *(Figura 1)*. Estos se pueden coordinar al mismo ligando (homoléptico) o a dos ligandos diferentes (heteroléptico) para facilitar la incorporación de tales iones adicionales. Los complejos heterometálicos derivados podrían desempeñar un papel importante en la computación cuántica con la unidad de Fe(II) actuando como un interruptor molecular y los metales externos como bits cuánticos.

Para lograr este objetivo, se ha llevado a cabo la síntesis y caracterización de diferentes ligandos orgánicos. Además, se ha estudiado la capacidad de coordinación potencial de uno de ellos para producir complejos de Fe (II).

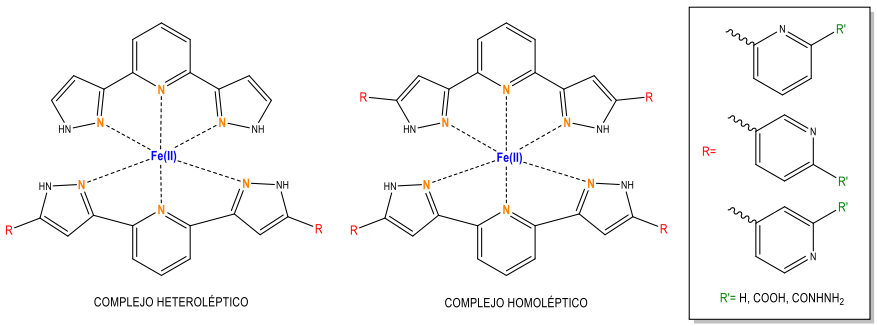

Figura 1. Complejos heterolépticos y homolépticos que contienen una unidad central de coordinación y unidades de coordinación externa.

Palabras clave: Transición de espín, química de coordinación, complejos de Fe(II), ligandos orgánicos, metaloligandos, computación cuántica, interruptores moleculares.

3. INTRODUCTION

3.1. COORDINATION CHEMISTRY

Crystal field theory is a model that explains the splitting of the orbitals of transition metals based on the repulsions between the ligands and the metal(s) that form the coordination complex (*Figure 2a*). In the case of d-orbitals the repulsions are asymmetric and hence they are split into two energy levels, e_g and t_{2g}. The energy between this two energy levels is named crystal-field splitting parameter (Δ), and for an octahedral environment is represented by Δ_{oct} *(Figure 2b).*

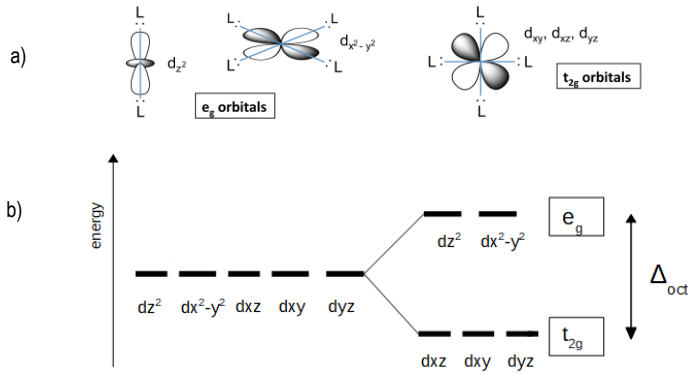

Figure 2. a) Asymmetric interaction between ligands and metal d-orbitals. b) Splitting of the metal d-orbitals when the metal is coordinated to the ligands in an octahedral environment.

The nature of Δ_{oct} depends on the deformation of the d orbitals when the ligand coordinate the metal. High values of crystal-field splitting parameter can be related to a high deformation of such orbitals. Spectrochemical series orders ligands and metals by the size of Δ that they produce by how much the ligands deform the d-orbitals and how affects the oxidation state of the metal to this deformation. Electrons of the transition metal complexes with an electronic configuration d^4-d^7 can be distributed in different ways, high spin, low spin or intermediate configurations *(Figure 3)*. Metallic ions of complexes can exhibit one of these electronic states depending on the balance between the electronic repulsion (P) and the crystal-field splitting parameter (Δ_{oct}).

When Δ_{oct}>P the preferential electronic configuration corresponds to the maximum spin pairing, thus a low spin (LS) state. When Δ_{oct}<P the preferential electronic configuration corresponds to the maximum spin unpaired, deriving in a high spin (HS) state. However in some cases, P is so close to Δ_{oct} that consequently can be achieved a switch between LS to HS and vice versa by application of an external perturbation. A behaviour named Spin CrossOver (SCO).

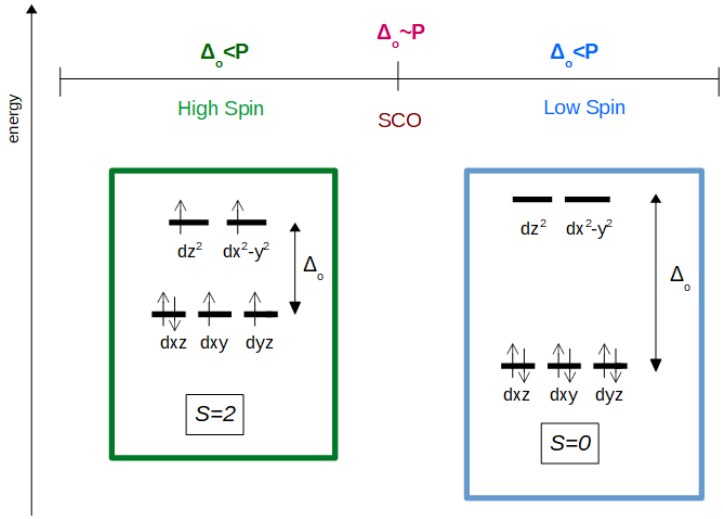

Figure 3. High spin, SCO and low spin electronic distribution in a d^6 metal within an octahedral environment.

3.2. Spin CrossOver (SCO)

The Spin CrossOver (SCO) is a behaviour owned to some first row transition metals with $3d^4$-$3d^7$ electronic configuration. This particular behaviour has been observed, for example, in Fe(II), Fe(III) and Co(II) ions.[1] It is also important the ligands involved in the complex. The SCO phenomenon is most commonly observed in Fe(II) complexes containing six nitrogen donor atoms, giving rise to a situation where P is close to Δ_{oct}.[2] Thus, one complex could exhibit SCO behaviour if it is formed by metals and ligands which are in the middle of the spectrochemical series, to assure a middle value of Δ_{oct} (fulfilling P close to Δ_{oct}). The spin state of SCO compounds changes due to the application of an external perturbation such as a variation of temperature, light irradiation, pressure, magnetic field or insertion of a guest molecule into the system. Temperature variation is the most common method to switch between the spin states. The

thermal-induced SCO behaviour can be studied by representing the fraction of metal ions that are in the HS state (γ_{HS}) versus temperature *(Figure 4)*. The temperature at which half of the metal centres are in either state is named $T_{1/2}$.

The shape of these curves displays the three possible behaviours observed in consequence of the cooperativity of the complex. The degree of cooperativity arises from intermolecular interactions and refers to the propagation of the structural and electronic changes within the crystal lattice.[3] Three strategies could increase cooperativity within SCO compounds: i) link the SCO centres, as in polymers, ii) induce hydrogen bonding via the ligands and iii) favour the formation of π··· π interactions.[1] The higher cooperativity leads to a more abrupt transition, and when it is particularly high it can induce hysteresis.

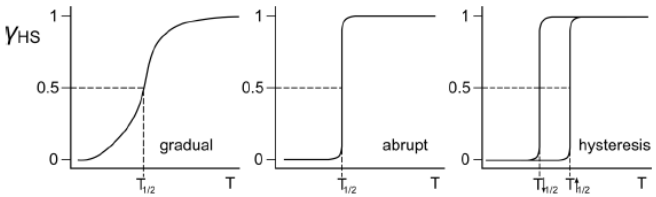

Figure 4. Representation of γ_{HS} versus temperature in different SCO behaviours in consequence of cooperativity.

In the first curve, the transition is gradual and the switch between both states takes place in a wide temperature range, indicating that not all metal centres within the complex are undergoing the transition at the same temperature. In the second curve, an abrupt transition occurs and the SCO process takes place in a narrower range of temperatures. The third curve presents hysteresis, where there are two values of $T_{1/2}$ (one belonging to the cooling mode and the other belonging to the heating mode). This last scenario leads to a bi-stable region, where the spin states are in equilibrium, so there is a co-existence of two spin states at the same temperature. Hysteresis system is the most desirable system as it can be very useful for technological applications.

3.3. Fe(II) Complexes

As it has been explained above, complexes could contain SCO behaviour if they are formed by metals and ligands which are in the middle of the spectrochemical series. Therefore, good examples of SCO systems are those which have Fe(II) and organic ligands containing nitrogen coordinating atoms. In that sense, 2,6-bis(pyrazol-3-yl)pyridine (3-bpp) derivative ligands are a good example, such as those synthesised by GMMF group.[4,5]

Our strategy is based on Fe(II) compounds constructed with other type of 3-bpp derivatives ligands, either homoleptic or heteroleptic, exhibiting coordinating unities on the external part of the ligands, where additional transition metals or lanthanides can be coordinated in. These additional coordinating units are formed by nitrogen groups together with H, COOH or $CONHNH_2$ units, the nitrogen donor atom being placed in different possible positions *(Figure 5)*.

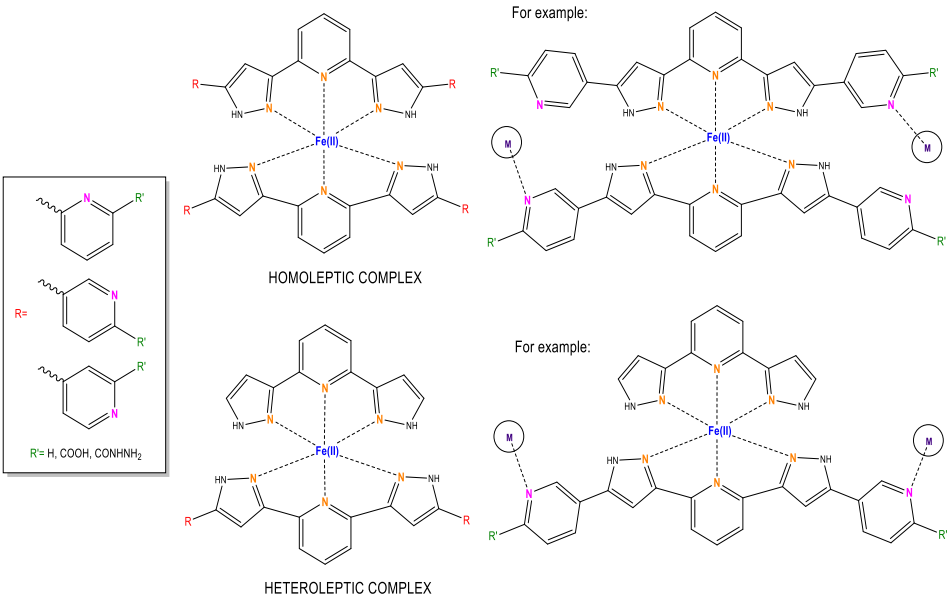

Figure 5. Complexes which present SCO behavior and which can further produce heterometallic systems.

The central part of the complex, formed by Fe(II) and the 3-bpp coordination sphere, allows the system to show SCO behaviour. The external parts of the ligands are expected to allow other metals to be coordinated in (*Figure 5*).

The interest behind this type of molecular architecture is that the iron(II) might have the ability to activate/deactivate the possible interaction between the external metals due to the inherent bistability (HS and LS) achieved by the abrupt spin transitions with hysteresis by increasing the cooperativity. In fact, the SCO phenomenon has potential uses as switches, data storage devices and optical displays.

4. OBJECTIVES

This new research line will be based on the synthesis, characterization and study of iron(II) compounds that exhibit additional coordinating units. First, a previous study of the Fe(II) complexes is necessary to verify its properties as a switch, due to SCO phenomenon, then the additional units would be exploited to explore the coordination of other metals in the complex.

To achieve this principal goal, several sub-objectives will be fulfilled:

· Synthesis of 3-bpp derivative ligands. Characterization by nuclear magnetic resonance, mass spectrometry and infrared spectroscopy.

· Synthesis of new iron (II) coordination complexes in different conditions. Characterization by single-crystal X-ray diffraction, mass spectrometry and infrared spectroscopy.

5. DISCUSSION OF RESULTS

The design of new complexes featuring SCO properties and external coordinating units depends on the synthesis of new organic ligands derived from 3-bpp and it also depends on finding a satisfactory crystallization conditions for the complexes.

5.1 DESIGN OF 3-BPP DERIVATIVES

The synthesis of new organic ligands derived from 3-bpp, which contain central nitrogen donor atoms which promote SCO behaviour and external groups with additional donor atoms, has been carried out in this project. These ligands have been synthesized in a particular order, starting from the simplest one and following with more complex ligands.

The first proposal is 2,6-bis(5-(pyridin-2-yl)-1H-pyrazol-3-yl)pyridine ligand, named H_2L1 (*Figure 6*). This ligand has been synthesised previously in GMMF research group, as well as in another research group.[6] However, it potential to promote Fe(II) SCO complexes has never been explored. Moreover, it is interesting for this project, since the synthesis procedure is already known and thus is a good starting point to take hands-on experience, and to compare its potential coordination capabilities with other more complex 3-bpp derivative ligands.

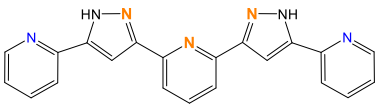

Figure 6. H_2L1 ligand

The second proposal is 2,6-bis(5-(pyridin-3-yl)-1H-pyrazol-3-yl)pyridine, named H_2L2 (*Figure 7*). What is interesting of this ligand is the external nitrogen, which is in the *meta* position to the pyrazole and it allows an easier coordination to additional metals, since there will be less steric hindrance if a metal is coordinated to the nitrogen in H_2L2 than in H_2L1.

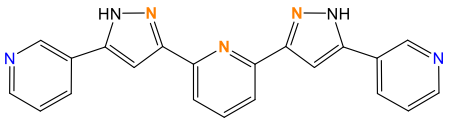

Figure 7. H_2L2 ligand

The third proposal is 5,5'-(pyridine-2,6-diylbis(1H-pyrazole-3,5-diyl))dipicolinic acid, named H_4L3 (*Figure 8*). This ligand differs from H_2L1 and H_2L2 by the carboxylic acid in *para* position to the pyrazole. The picolinate group can act as a bidentate chelating agent of metal ions and can also compensate the additional charge of the metal ion. Actually, some studies indicate that metal is coordinated through one of the COO^- oxygen donor atoms and the pyridinic nitrogen.[7]

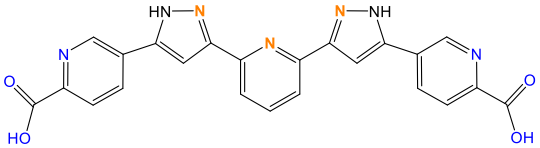

Figure 8. H_4L3 ligand

The final proposal is 3,3'-(pyridine-2,6-diylbis(1H-pyrazole-3,5diyl))di(benzohydrazide), named H_4L4 (*Figure 9*). This ligand contains a hydrazide acid group, which can act as a bidentate ligand, chelating other metal ions, as H_4L3. Some studies indicate that the coordination to a metal occurs through the carbonyl oxygen and amine nitrogen.[8]

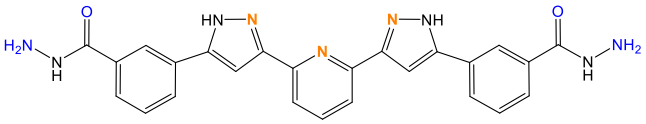

Figure 9. H_4L4 ligand

5.1.1 Preparation and characterization of ligands

5.1.1.1 Synthesis of 2,6-bis(5-(pyridin-2-yl)-1H-pyrazol-3-yl)pyridine (H_2L1)

H_2L1 was synthesised from 2,6-pyridinedicarboxylic acid (4) and it was prepared in three stages (*Figure 10*). The first stage is an esterification, where 2,6-pyridinedicarboxylic acid (4) is transformed in diethyl 2,6-pyridinedicarboxylate (3). The second stage (in the dashed box) consists in a Crossed Claisen condensation between 2-acetylpyridine and diethyl 2,6-pyridinedicarboxylate (3), which form a β-diketone (H_2LA, 2). The third stage is a ring closing reaction, where the β-diketone forms a pyrazole. In this last stage, the H_2L1 ligand (1) is obtained.

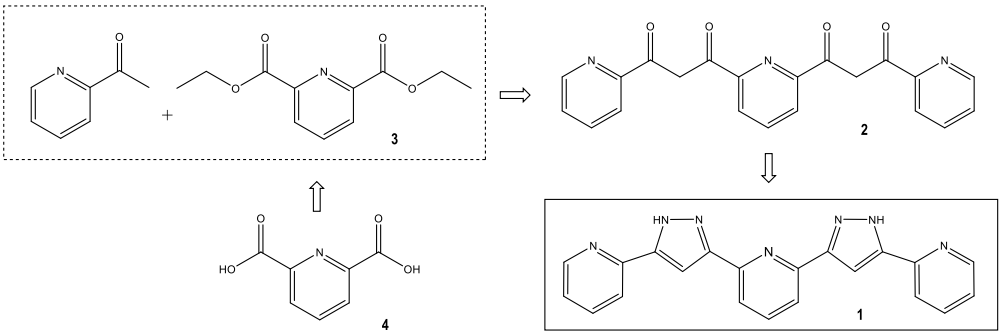

Figure 10. Synthetic route of H_2L1

First Stage: Synthesis of diethyl 2,6-pyridinedicarboxylate

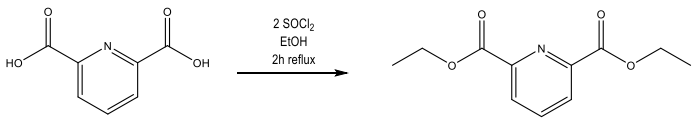

Figure 11. Synthesis of diethyl 2,6-pyridinedicarboxylate

This first stage is an esterification (*Figure 11*). Hydroxyl group is a bad leaving group, however it is replaced by a chloride through a nucleophilic substitution, addition-elimination mechanism, forming an acyl chloride, which is a better leaving group and it allows a new nucleophilic substitution by the methoxide group from methanol.

Diethyl 2,6-pyridinedicarboxylate was characterized by ^{1}H NMR in $CDCl_3$. This technique shows the purity of the compound, since all signals obtained in the spectrum are identified and assigned (*Figure 12*).

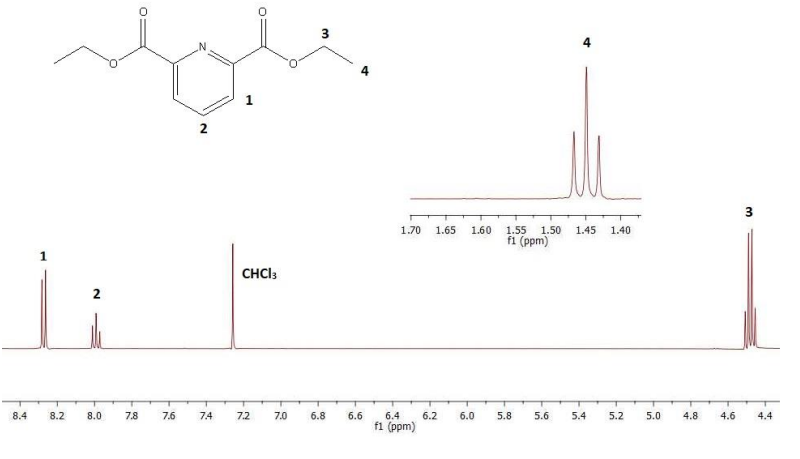

Figure 12. ^{1}H-NMR of diethyl 2,6-pyridinedicarboxylate

Second Stage: Synthesis of 1,3-bis-(3-oxo-3-(2-pyridyl)propionyl)pyridine (H_2LA)

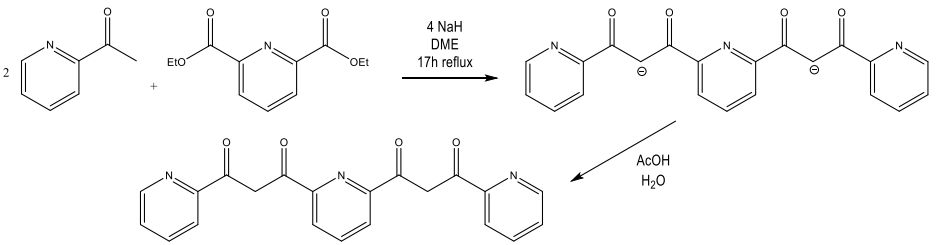

Figure 13. Synthesis of H_2LA

This second stage is a crossed Claisen condensation between an enolizable ketone (2-acetylpyridine) and a nonenolizable ester (diethyl 2,6-pyridinedicarboxylate) where a strong base removes a proton from the ketone which attacks the carbonyl carbon of the ester giving place a nucleophilic substitution (*Figure 13*). This reaction was carried out under N_2 atmosphere, due to the violent exothermic reaction between NaH and environmental humidity. NaH was added to a solution of 2-acetylpyridine and diethyl 2,6-pyridinedicarboxylate in DME, since only the ketone is enolizable, so only the ketone is deprotonated. Due to the acidity of the protons between the

diketone, the NaH base promotes the deprotonated ligand. Then, it is protonated by adding an acid.

H_2LA ligand exhibits keto-enol tautomerism (*Figure 14*), where an equilibrium between the keto form and the enol form is achieved by the movement of the alpha hydrogen atoms and the shifting of bonding electrons.

Figure 14. keto-enol tautomerism of H_2LA

H_2LA was characterized by ^1H NMR in $CDCl_3$ (*Figure 15*). The spectrum suggests that in this medium and at room temperature the equilibrium is not reached and the ligand exhibits its enolic form. The spectrum is as expected and signals are identified bellow.

Figure 15. ^1H-NMR of H_2LA

H_2LA was also characterized by electrospray ionization mass spectrometry (*Figure 16*). The mass spectrum is as expected. The most intense signal is 374.11 which correspond to $[M+H]^+$.

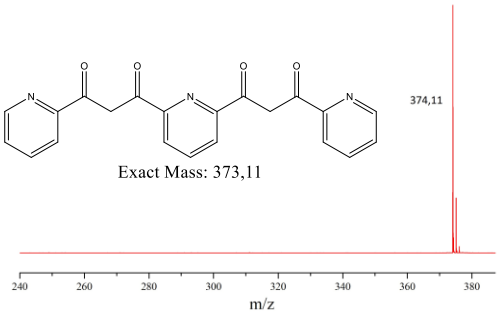

Figure 16. Selected region of the mass spectrum of H_2LA

Third Stage: Synthesis of 2,6-bis(5-(pyridin-2-yl)-1H-pyrazol-3-yl)pyridine (H_2L1)

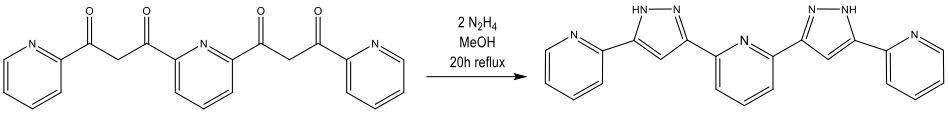

Figure 17. Synthesis of H_2L1

The third stage is the ring closing reaction, where both β-diketone units from H_2LA react with hydrazine to give five-membered heterocycles known as a pyrazoles (*Figure 17*).
The hydrazine makes a nucleophilic attack to the carbonyl carbon of one ketone and by imine mechanism, an imine is formed. Then, the other hydrazine nitrogen makes a nucleophilic attack to the carbonyl carbon of the other ketone, forming a five membered ring which by an electron reorganization forms an aromatic pyrazole.

H_2L1 was characterized by ^1H NMR in DMSO (*Figure 18*). This spectrum, although exhibiting broad signals, is as expected and those signals are identified bellow.

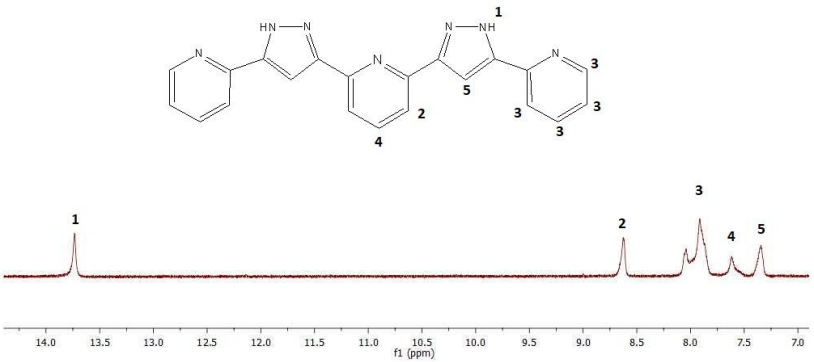

Figure 18. ^1H-NMR of H_2L1

5.1.1.2. Synthesis of 2,6 bis(5-(pyridin-3-yl)-1H-pyrazol-3-yl)pyridine (H_2L2)

H_2L2 was synthesised from 2,6-pyridinedicarboxylic acid (4) and it was prepared in three stages similarly to H_2L1 (*Figure 19*). The first stage is an esterification, where 2,6-pyridinedicarboxylic acid (4) is transformed in diethyl 2,6-pyridinedicarboxylate (3). The second

stage (in the dashed box) consists in the crossed Claisen condensation between 3-acetylpyridine and diethyl 2,6-pyridinedicarboxylate (3), which form a bis-β-diketone molecule (H_2LB, 2). The third stage is the ring closing reaction, where the β-diketone units form pyrazoles producing the H_2L2 ligand (1) is obtained.

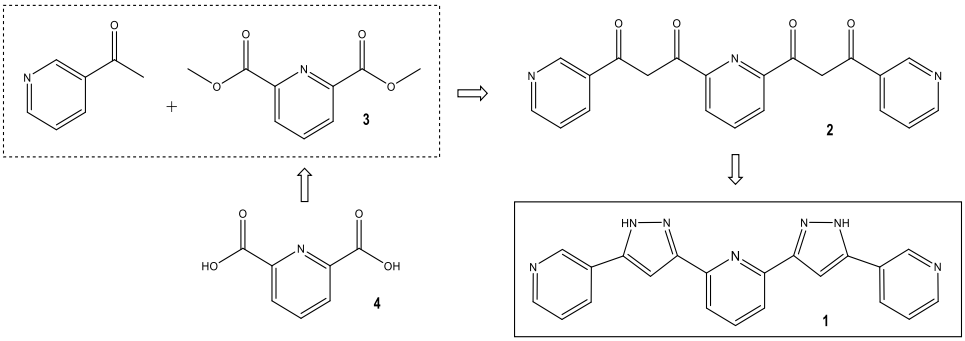

Figure 19. Synthetic route of H_2L2

First Stage: Synthesis of diethyl 2,6-pyridinedicarboxylate

The starting material was obtained as previously in the first stage of the H_2L1 synthesis.

Second Stage: Synthesis of 3,3'-(pyridine-2,6-diyl)bis(1-(pyridin-3-yl)propane-1,3-dione) (H_2LB)

First Approach

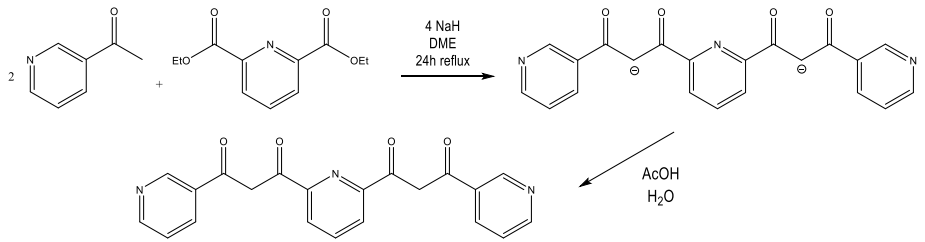

Figure 20. Synthesis of H_2LB, first approach

In the second stage, two different approaches have been carried out. The first one, consists in the crossed Claisen condensation between an enolizable ketone (3-acetylpyridine) and a nonenolizable ester (diethyl 2,6-pyridinedicarboxylate) (*Figure 20*), using DME and NaH as reagents and thus following the same procedure as in the second stage of H_2L1 synthesis.

H_2LB was characterized by ^1H NMR in DMSO (*Annex, 1*). The spectrum shows more signals than expected, with a broad character that precludes its analysis. Thus, mass spectrometry was carried out to explore the nature of the molecule (*Figure 21*). The most intense signal is 374,11 which correspond to $[M+H]^+$ and the 271,11 signal corresponds to a new unexpected product.

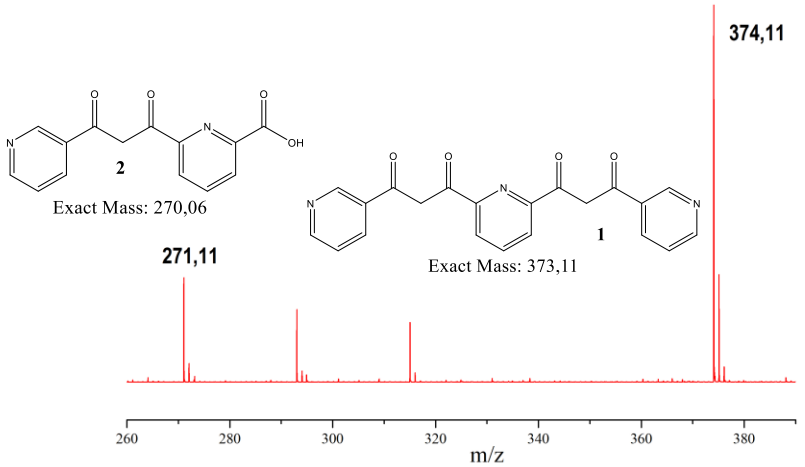

Figure 21. Selected region of the mass spectrum of H_2LB

Mass spectrum indicates the existence of H_2LB (1) as the main product, but also the signal corresponding to 6-(3-oxo-3-(pyridin-3-yl)propanoyl)picolinic acid (2) compound. One possibility for the formation of this unexpected product could be due to a retro-Claisen cleavage where the β-diketone reacts with the excess of NaH base and the traces of water in the medium, causing a fragmentation. It should be noted that he pyridinic nitrogen atoms attract de electronic density of the β-diketone units, leading to a more electrophilic carbonyl, which increases the possibility of the occurrence of the retro-Claisen cleavage. A second approach has been realized to try to avoid the retro-Claisen cleavage.

Second Approach

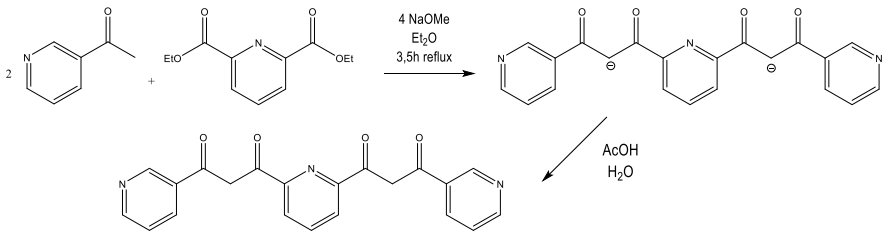

Figure 22. Synthesis of H_2LB, second approach

In this second approach, the same Claisen condensation is performed but the base used is NaOMe in Et_2O instead of NaH in DME (*Figure 22*). These new conditions were chosen since the boiling temperature of Et_2O is lower than that of DME, allowing softer reaction conditions in order to avoid the H_2LB ligand to suffer the retro-Claisen reaction. Also, the reaction time was reduced significantly (from 24 to 4 hours).

The H_2LB solid obtained in this second approach was characterized by ^1H NMR in $CDCl_3$. The spectrum suggests that the retro-Claisen cleavage has not occurred in the same amount as in the first approach, since H_2LB synthesized from second approach is of a better quality than H_2LB from first approach. ^1H NMR spectrum is as expected and signals are identified in *Annex, 2.*

Third Stage: Synthesis of 2,6-bis(5-(pyridin-3-yl)-1H-pyrazol-3-yl)pyridine (H_2L2)

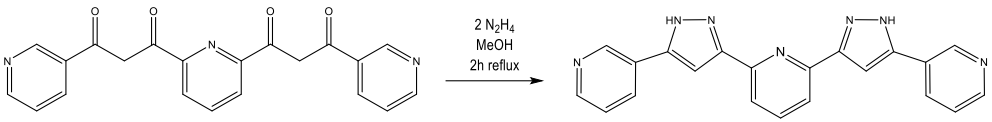

Figure 23. Synthesis of H_2L2

The third stage is a ring closing reaction (*Figure 23*) where a five-membered pyrazole is formed, as explained previously in H_2L1 synthesis. In this case, the H_2LB product obtained from the first approach was used, to explore the closing ring procedure of the molecules obtained.

The final product was characterized by ^1H NMR in DMSO (*Annex, 3*). As expected, mass spectrum (*Figure 24*) indicates the existence of two species, H_2L2 (1) and 6-(5-(pyridin-3-yl)-1H-pyrazol-3-yl)picolinic acid (2), corresponding to the two products obtained in the first approach of H_2LB. When the ring closing reaction has been carried out, all the β-diketone have been cycled, forming again two products.

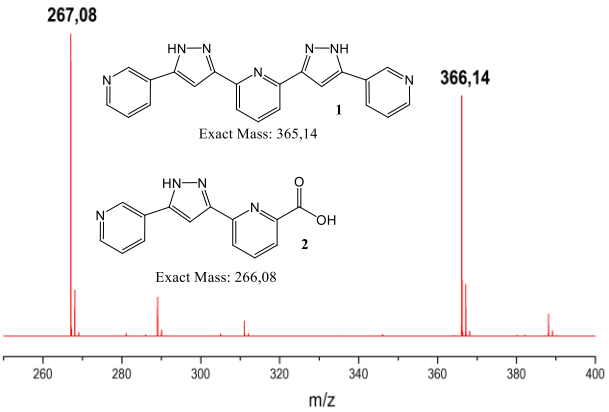

Figure 24. Selected region of the mass spectrum of H_2L2

5.1.1.3. Synthesis and characterization of 5,5'-(pyridine-2,6-diylbis(1H-pyrazole-3,5-diyl))dipicolinic acid (H_4L3)

The synthetic route of H_2L3 is shown in *Figure 25*. The first stage is an esterification, which forms dimethyl pyridine-2,5-dicarboxylate (4) from 2,5-pyridinedicarboxilic acid (5). The second stage is the formation of the 5-(methoxycarbonyl)picolinic acid (3) by a half hydrolysis of the ester (4). The third stage (in the dashed box) is the corresponding Crossed Claisen condensation between 2,6-diacetylpyridine and 5-(methoxycarbonyl)picolinic acid (3), which forms a bis-β-diketone molecule (H_2LC, 2). The third stage is a ring closing reaction, where each β-diketone forms a pyrazole. In this last stage the H_4L3 ligand (1) is obtained.

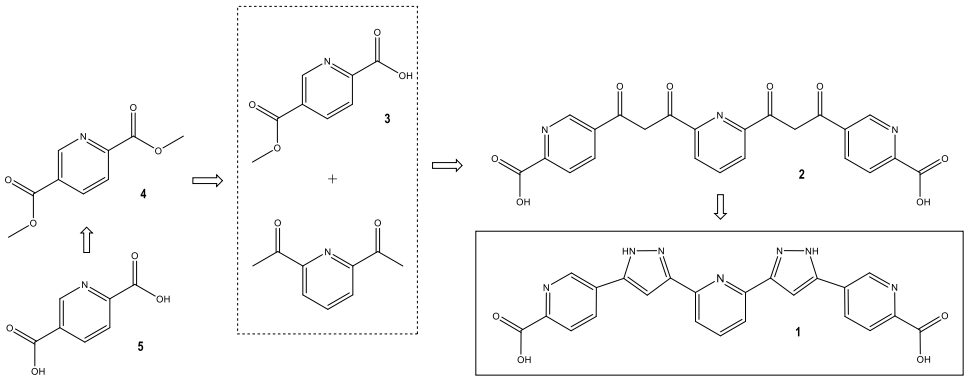

Figure 25. Synthetic route of H_4L3

First Stage: Synthesis of dimethyl 2,5-pyridinedicarboxylate

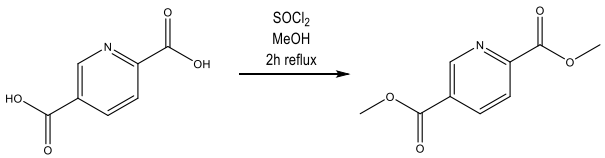

Figure 26. Synthesis of dimethyl 2,5-pyridinedicarboxylate

The first stage (*Figure 26*) is an esterification as explained previously. Dimethyl 2,5-pyridinedicarboxylate was characterized by ^1H NMR in $CDCl_3$ (*Figure 27*). This technique shows the purity of the compound. The spectrum is as expected and signals are identified bellow.

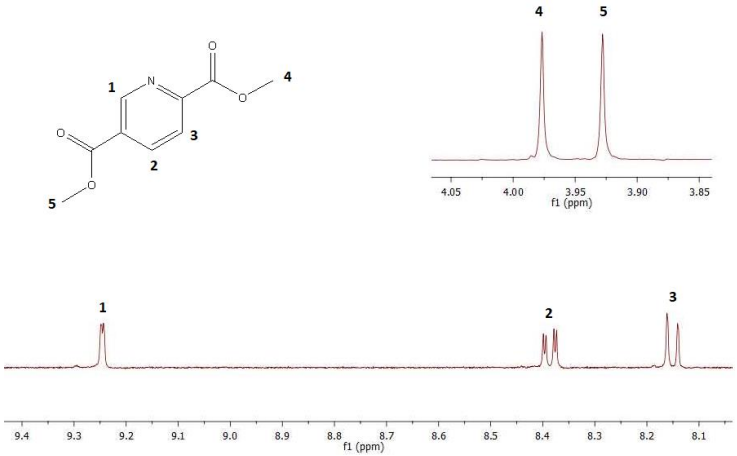

Figure 27. ^{1}H-NMR of dimethyl 2,5-pyridinedicarboxylate

Second Stage: Synthesis of dimethyl 5-(methoxycarbonyl)picolinic acid

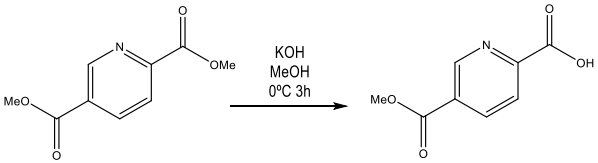

Figure 28. Synthesis of dimethyl 5-(methoxycarbonyl)picolinic acid

The second stage (*Figure 28*) is a half base-catalysed ester hydrolysis of dimethyl 2,5-pyridinedicarboxylate by an addition-elimination mechanism. Previously it was reported the half hydrolysis of diethyl 2,6-pyridinedicarboxylate under this conditions,[9] but in our case it is unknown which methyl ester would be attacked first.

In order to explore this reaction, the same procedure was followed, using KOH as base and MeOH at 0° C. The product obtained was characterized by ^{1}H NMR in CD_3CD (*Annex, 4*). This technique shows the hydrolysis of the two methyl esters, and thus that the reaction did not take place. An alternative H_4L3 synthesis route has been proposed and explained bellow.

Alternative H_4L3 synthesis route

An alternative synthesis route of H_4L3 is shown in *Figure 29*. The first reaction is a Fischer esterification, as seen above in the synthesis of dimethyl 2,5-pyridinedicarboxylate, where 6-methylnicotinic acid (5) is converted to methyl 6-methylnicotinate (4). In the dashed box is shown the consequently crossed-Claisen condensation between an enolizable ketone, 2,6-diacetylpyridine and the nonenolizable ester methyl 6-methylnicotinate (4), forming the bis-β-diketone molecule (3). The next reaction is based on closing the β-diketone with hydrazine to give the five-membered heterocycles, pyrazoles. The last reaction is an oxidation of an aromatic alkane with $KMnO_4$, which allows the methyl be converted into a carboxylic acid. However, it is not known how $KMnO_4$ oxidative agent is going to affect the pyrazole group. This feature, as well as the synthetic route, could be studied in the future.

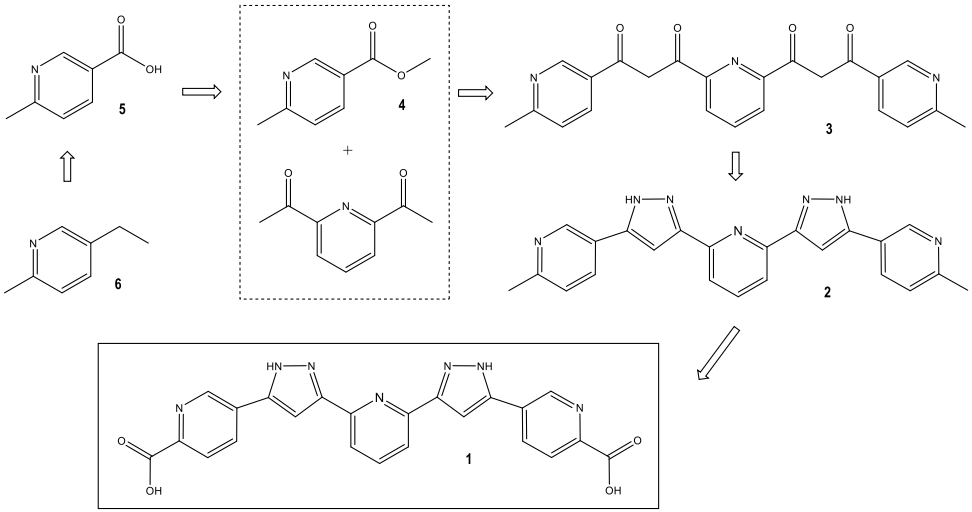

Figure 29. Alternative synthesis route of H_4L3

5.1.1.4. Synthesis and characterization of 3,3'-(pyridine-2,6-diylbis(1H-pyrazole-3,5-diyl))di(benzohydrazide) (H_4L4)

A proposal to the synthesis of H_4L4 is shown in *Figure 30*. The first stage (in a dashed box) is a crossed-Claisen condensation between 2,6-diacetylpyridine and dimethyl isophthalate (3), which could form a bis-β-diketone molecule (H_2LD, 2).The third stage is the ring closing reaction, where the β-diketone units form pyrazoles, and the external methyl esters form acylhydrazine groups in the external part of the ligand.[10]

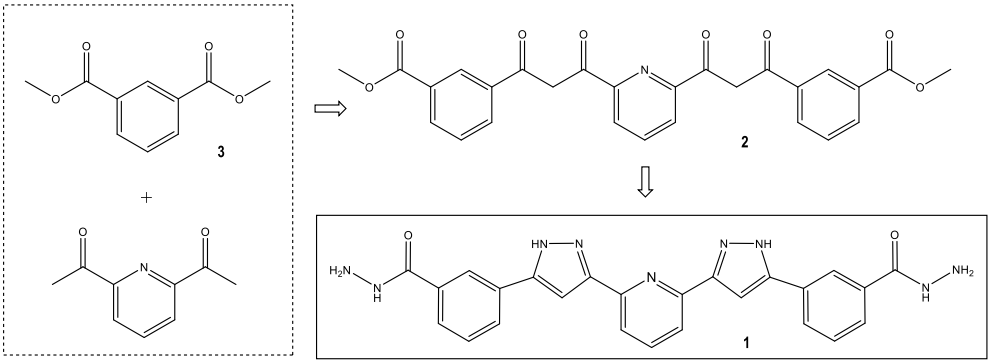

Figure 30. Synthesis route of H_4L4

First Stage: Synthesis of dimethyl 3,3'-(3,3'-(pyridine-2,6-diyl)bis(3-oxopropanoyl)) dibenzoate (H_2LD)

First Approach

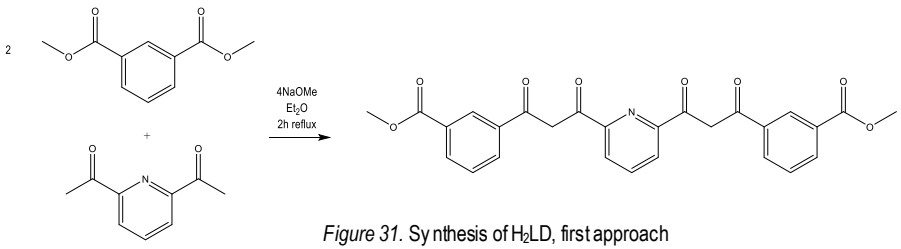

Figure 31. Synthesis of H_2LD, first approach

In the first stage of the first attempt there is a Crossed Claisen condensation between an enolizable ketone, 2,6-diacetylpyridine and a nonenolizable ester, dimethyl isophthalate

(*Figure 31*). Following this approach, we expect each diester molecule to be condensed to each part of the 2,6-diacetylpyridine molecule. Soft conditions using short reaction times and low temperatures were carried out using Et_2O and sodium methoxide to deprotonate 2,6-diacetylpyridine, followed by the addition of the diester unit.

Two different solids were obtained under these conditions, one being insoluble. The soluble brown solid obtained was characterized by ^1H NMR in $CDCl_3$, (*Annex, 5*). This technique shows there are not aromatic hydrogen atoms, hence, this spectrum shows that the product is not the expected one. Thus, the unsoluble solid should exhibit the aromatic groups of the starting material, although not being soluble. A possible explanation for this fact could be found considering the experimental procedure followed in this attempt. The NaOMe base forms the enolate of 2,6-diacetylpyridine and it is in excess in the flask. Then, dimethyl isophthalate is added, being in defect. Thus, the deprotonated 2,6-diacetylpyridine attacks the dimethyl isophthalate and one molecule of H_2LD is formed. However, H_2LD has also an ester in its structure, which allows the deprotonated 2,6-diacetylpyridine (in excess) to further attack H_2LD forming an oligomer, as shown in *Figure 32*. As an alternative to this fact, it has been proposed a different experimental procedure, the second approach bellow.

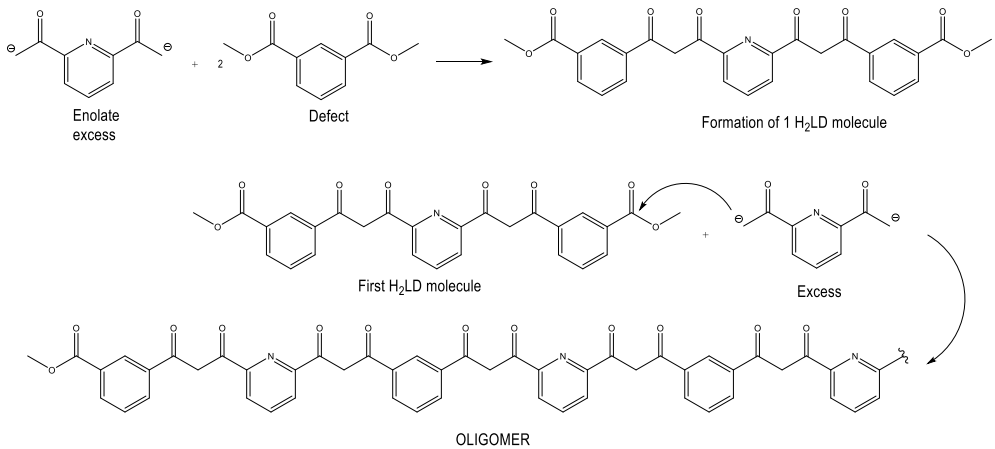

Figure 32. Oligomerization of H_2LD

Second Approach

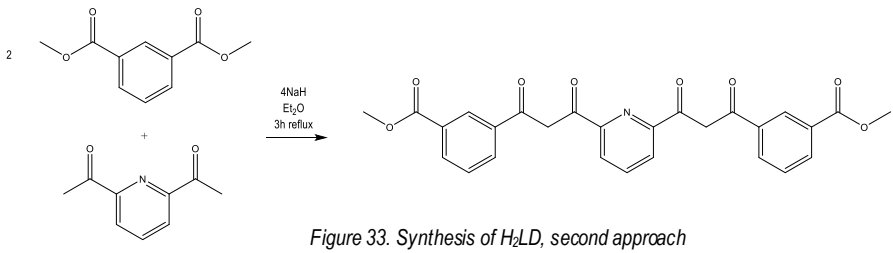

Figure 33. Synthesis of H_2LD, second approach

The second approach is the same crossed-Claisen condensation, but changing the order of addition of starting materials (*Figure 33*). There is an addition of 2,6-diacetylpyridine, previously deprotonated with NaH, to a dimethyl isophthalate solution. Thus, dimethyl isophthalate is in excess and 2,6-diacetylpyridine enolate is in defect. The enolate which is in defect attack the dimethyl ester instead of the formed H_2LD. The solid obtained under these conditions was characterized by ^1H NMR in $CDCl_3$ (*Annex, 6*). However, there are several broad signals and the spectrum is not conclusive.

5.2. STUDY OF HOMOLEPTIC COMPLEXES

The design of new complexes featuring SCO properties and which can act as metaloligands depends on finding a satisfactory crystallization conditions for the complexes. From the current experience of the GMMF research group on these systems, it is known that long periods are required for the compounds to crystallize (3-6 weeks).

In this project, the coordination has been carried out with the ligand H_2L1 and iron (II) as metal. The expected complex is shown in *Figure 34.*

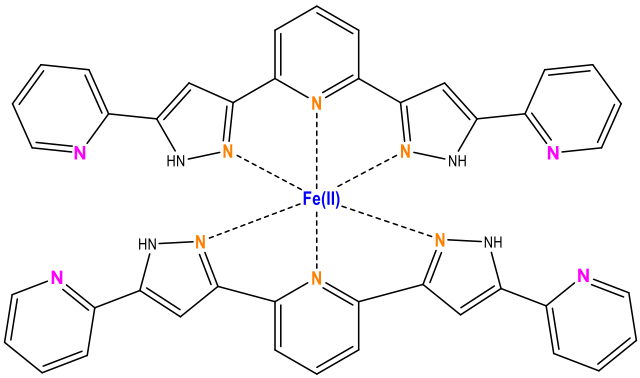

Figure 34. Expected complex from the reaction bellow

5.2.1 Synthesis of coordination complexes

The synthesis of the Fe(II) homoleptic complex, performed in different steps is based in this general procedure;

$$2\ H_2L1 + Fe(II)\ salt \rightarrow [Fe(H_2L1)_2]^{2+}$$

Where the stoichiometric amount of ligand is used to encapsulate one Fe(II) ion. In the experimental procedure, it is important the addition of the ligand to the Fe(II) salt solution, since the resulting products were more soluble in the reaction media thus facilitating the crystallization methods. Fe(II) can be oxidised easily, thus it is convenient to add ascorbic acid to the solution or perform the reaction in a glove box, to avoid the iron(II) oxidation to Fe(III). When the reaction has finished, if a solution is obtained it is layered with different antisolvents to crystallize the product of the reaction. If a suspension is obtained, it is filtered and the solid obtained is solved again in another solvent, normally DMF, and then this solution is layered with different

antisolvents. It should be noted that the antisolvent is miscible with the reaction solvent but has different density, which allows to make two layers that slowly diffuse. This diffusion makes less soluble the environment of the complex and this induces crystallization.

The complexes syntheses are explained in part 6.2.1, showing all the different reaction conditions used. In the table below (*Table 1*), it is displayed all the reactions performed with the ligand H_2L1 and Fe(II) in different conditions and the result obtained.

Entry	Fe(II) salt	Antioxidant	Reaction solvent	Solution solvent	Antisolvent	Result
CV16	$Fe(ClO_4)_2 \cdot XH_2O$	AA	MeOH	DMF	Acetone	Orange solution
					THF	Amorphous solid
					Et_2O	Amorphous solid
CV17	$Fe(ClO_4)_2 \cdot XH_2O$	AA	Acetone	DMF	Acetone	Orange solution
					Et_2O	Little red crystals
CV18	$Fe(ClO_4)_2 \cdot XH_2O$	AA	THF	-	-	-
CV19	$Fe(ClO_4)_2 \cdot XH_2O$	AA	$MeNO_2$	-	Acetone	Orange solution
					MeOH	Orange solution
CV20	$Fe(ClO_4)_2 \cdot XH_2O$	AA	MeOH	DMF	Acetone	Little red crystals
					THF	Little red crystals
					Et_2O	Little red crystals
CV21	$Fe(ClO_4)_2 \cdot XH_2O$	AA	$MeNO_2$	-	-	-
CV22	$Fe(ClO_4)_2 \cdot XH_2O$	AA	MeOH	-	-	-
CV24	$Fe(ClO_4)_2 \cdot XH_2O$	AA	1-propanol	DMF	Et_2O	Little red crystals
CV25	$Fe(ClO_4)_2 \cdot XH_2O$	AA	EtOH	DMF	Et_2O	Little red crystals
CV26	$Fe(ClO_4)_2 \cdot XH_2O$	AA	$MeNO_2$:MeOH	-	Acetone	Amorphous solid
					Et_2O	Amorphous solid
CV27	$[Fe(BF_4)_2] \cdot 6H_2O$	AA	MeOH	DMF	Et_2O	Little red crystals
CV29	$FeSO_4$	AA	MeOH	DMF	Et_2O	Little red crystals
CV30	$FeCl_2 \cdot 4H_2O$	AA	MeOH	DMF	Et_2O	Red crystals
CV31	$[Fe(BF_4)_2] \cdot 6H_2O$	GB	DMF	-	MeOH	Amorphous solid

Table 1. Performed reactions with H_2L1 ligand: Entry CV16 to CV31

Entry	Fe(II) salt	Antioxidant	Reaction solvent	Solution solvent	Antisolvent	Result
CV32	$[Fe(BF_4)_2]\cdot 6H_2O$	GB	Pyridine	-	Toluene	Amorphous solid
CV33	$[Fe(BF_4)_2]\cdot 6H_2O$	AA	Acetone	DMF	Et_2O	Red crystals
CV34	$[Fe(trifl)_2]\cdot 6H_2O$	AA	Acetone	DMF	Et_2O	Little red crystals
CV35	$Fe(AcO)_2$	AA	Acetone	-	-	-
CV36	$FeCl_2\cdot 4H_2O$	AA	Acetone	DMF	Et_2O	Amorphous solid
					MeOH	Amorphous solid

Table 1. Performed reactions with H_2L1 ligand: Entry CV32 to CV36

5.2.2 Structure and crystal lattice

During this project many attempts have been carried out (*Table 1*). Several of them did not crystalize and some of them produced non-single crystal or directly these single crystals did not exhibit enough quality to make possible the resolution of the structure by X-Ray diffraction. Among all crystals obtained, one of them exhibit enough quality to solve its structure (entry CV30).

5.2.2.1. Structure of $[Fe(H_2L1')_2]$

The single crystal structure obtained is unexpected, since it is formed by iron(II) complex with an unexpected ligand (*Figure 35*) it contains a carboxylic acid in meta position to the pyrazole and the coordination would be produced through the oxygen donor atom, as it will be shown later.

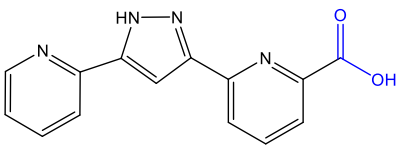

Figure 35. Unexpected ligand obtained from retro-Claisen cleavage (H_2L1')

H_2L1 was synthesised three times. Unfortunately for one of the batches obtained, the retro-Claisen cleavage occurred (explained in 5.1.1.2) leading the new ligand H2L1', as it is shown in *Figure 36*. It is important to mention that the two ligands, H_2L1 and H_2L1', were formed in the batch (as shown by the mass spectrum in *Figure 36*, carried out after obtaining the structure to

understand the origin of the new ligand) but in the coordination reactions there was a preference by the H_2L1' ligand.

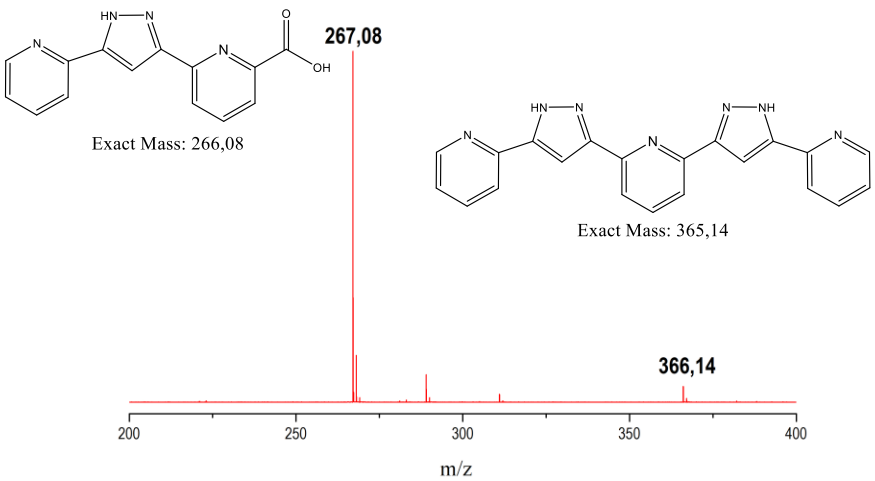

Figure 36. Selected region of the mass spectrum of H_2L1

Red crystals obtained in entry CV30 crystallize in the triclinic P-1 crystal system, where a≠b≠c and α≠β≠δ. The lattice parameters are shown in the table below (*Table 2*).

[Fe(H_2L1')$_2$] lattice parameters (100K)

a(Å):14.1439	α (º):99.301	V(Å^3): 2823.46
b(Å):14.6160	β(º):108.545	
c(Å):15.3161	δ(º):103.400	

Table 2. [Fe(H_2L1')$_2$] lattice parameters

The unit cell has two asymmetric units. Each asymmetric unit (*Figure 37,a*) is formed by two crystallographically independent iron(II) complexes (*Figure 37,b*).

Each complex has one iron (II) coordinated to a pyridinic nitrogen atom, to a pyrazole nitrogen atom and to a carboxylate unit, with an octahedral geometry (coordination number 6). Each iron(II) has different bonding distances, shown in table 3.

[Fe(H_2L1')$_2$] distance bonds (100K)

Fe(1)	Fe-N(pyridine)=2,12	Fe-N(pyrazole)=2,24	Fe-O(carboxylate)=2,14
Fe(2)	Fe-N(pyridine)=2,10	Fe-N(pyrazole)=2,23	Fe-O(carboxylate)=2,14

Table 3. [Fe(H_2L1')$_2$] distance bonds

Each ligand H2L1' is negative charged, given by the carboxylic group, thus the iron (II) charge is compensated. There are π···π interactions between the pyridine group of the parallel ligands of each iron (II) complex. There are also hydrogen bonding between the pyrazole NH group and the pyridine nitrogen and between pyrazole NH group and the methanol molecules that complete the structure filling holes.

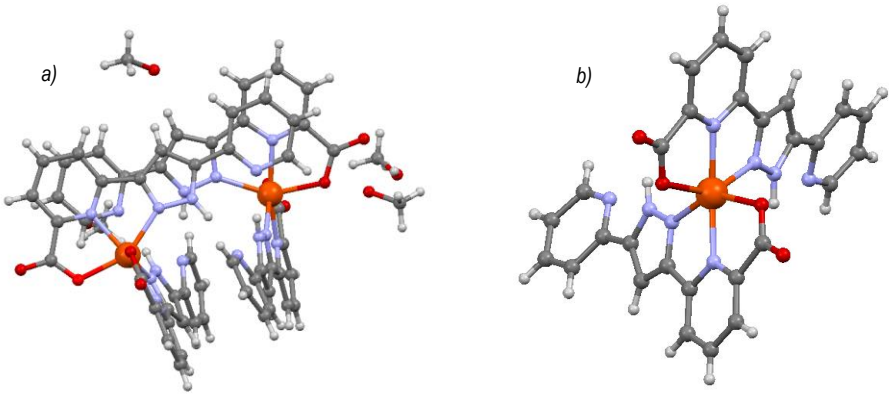

Figure 37. a) Asymmetric unit of [Fe(H_2L1')$_2$] b) [Fe(H_2L1')$_2$] complex

The H_2L1' ligand coordinated to the iron(II) by two nitrogens and one oxygen doesn't allow the complex to exhibit SCO properties. As it has been mentioned in the introduction, the SCO phenomenon is commonly observed in Fe(II) complexes containing ligands which cause a middle value of Δ_o (fulfilling P close to Δ_{oct}) and the carboxylate pocket does not fulfil this characteristic. In this system, temperature close to 100K, the Fe(II) complex exhibit HS, hence it is not possible to observe a spin transition.

6. EXPERIMENTAL SECTION

6.1. MATERIALS AND METHODS

Concerning to the instrumentation, reagents and solvents used in the development of the project have been provided by the GMMF research group.

6.1.1 Physical techniques

In other to characterize ligands and complexes, different physical techniques have been used:

· Single Cristal X-Ray Crystallography: Data of crystals were collected using a bruker APEX II CCD diffractometer on the Advanced Light Source beamline 11.2.1 at Lawrence Berkeley National Laboratory. .

· Nuclear Magnetic Resonance Spectroscopy: spectra were registered on a Varian Inova 300 MHz instrument at the "Unitat de RMN" of the Universitat de Barcelona.

· Mass Spectrometry: ESI mass spectrometry experiments were recorded at the "Unitat d'Espectrometria de Masses de Caracterització Molecular" of the Universitat de Barcelona by using a LC/MSD-TOF (Agilent Technologies) with a dual source with a lock spray for internal reference introduction.

6.2. SYNTHESIS OF LIGANDS

6.2.1 Synthesis of H_2L1

❖ First Stage: Synthesis of diethyl 2,6-pyridinedicarboxylate

To a solution of 2,6-pyridinedicarboxylic acid (5 g, 30 mmol) in EtOH (200 ml) was added dropwise thiolyl chloride (5.6 ml, 47 mmol) and was brought to reflux for two hours. The resulting colourless solution was allowed to cool to room temperature and the solution was carried to dryness in the rotary evaporator. To remove all HCl present in solution, extractions of $CHCl_3$ and water were carried out, until having pH=5 in the organic phase phase. The final product was obtained by removing all $CHCl_3$ in the rotary evaporator, as a white solid with 79% yield. This solid was characterized by ^1H NMR.

❖ Second Stage: Synthesis of H_2LA

A suspension of ethyl dipicolinate (5,33 g, 23.7 mmol) and 2-acetylpyridine (11,5 ml, 102,5 mmol) in DME (100 ml) was stirred under nitrogen atmosphere. NaH dispersion in mineral oil was suspended in hexane to remove this mineral oil, and then the pure NaH (4,97 g, 207,1 mmol) was added to 50 ml of DME. This NaH in DME suspension was added dropwise into the ethyl dipicolinate and 2-acetylpyridine suspension. The suspension turned dark red. Reflux was maintained for 17 hours. The NaH was quenched with EtOH (5 ml), until the absence of H_2 apparition. The resultant red salt was collected by filtration and suspended in H_2O (300 ml) then was added dropwise AcOH (9 ml) and the solution was stirred for 30 minutes. The solid was filtered, then was extracted in $CHCl_3/H_2O$. $CHCl_3$ phase was evaporated. A brown solid was obtained with 12% yield. This solid was characterized by ^1H NMR.

❖ Third Stage: Synthesis of H_2L1

To a solution of H_2LA (1.06 g, 2.8 mmol) in MeOH (120 ml) brown suspension was added hydrazine (2 ml, 26.8 mmol), and reflux was maintained for 20 hours. The volume of the resulting brown suspension was reduced to the half in the rotary evaporator. The resultant white product was filtered. The mother liquor was evaporated again to the half, and was carried to the refrigerator until obtaining all the solid possible. A white solid was obtained with 93% yield. This solid was characterized by ^1H NMR.

6.2.2 Synthesis of H_2L2

❖ First Stage: Synthesis of diethyl 2,6-pyridinedicarboxylate

The preparation and characterization of 2,6-pyridinedicarboxylate has been mentioned previously in the first stage of the synthesis of H_2L1.

❖ Second Stage: Synthesis of H_2LB

First Approach

A suspension of ethyl dipicolinate (3,1 g, 13,9 mmol) and 3-acetylpyridine (5,9 ml, 53,6 mmol) in DME (100 ml) was stirred under nitrogen atmosphere. NaH dispersion in mineral oil was suspended in hexane (30 ml) to remove this mineral oil, and then the pure NaH (2,7 g, 112,5 mmol) was added to 30 ml of DME. This NaH in DME suspension was added dropwise into the ethyl dipicolinate and 3-acetylpyridine suspension. The suspension turned white, then light yellow, and finally red. Reflux was maintained for 24 hours. The resulting red suspension was allowed to cool and excess NaH was quenched with EtOH (3,9 ml), until the absence of H_2 apparition. The resultant red salt was collected by filtration and suspended in H_2O (150 ml) then was added dropwise and gradually AcOH (10 ml) and the solution was stirred for 20 minutes. The light brown solid was filtered and washed with water, then was washed with Et_2O. The solid was suspended in THF (80 ml) and was added dropwise and gradually a saturated solution of $NaHCO_3$ (10 ml), this suspension was brought to reflux for 10 minutes. The resultant suspension was filtered and the solid was suspended in 50 ml of H_2O, and 10 ml of AcOH was added, then it was stirred for 15 minutes. This suspension was filtered and washed with water and Et_2O. A light brown solid was obtained with 12% yield. This solid was characterized by ^1H NMR.

Second Approach

MeOH (18 ml) is added dropwise and gradually to solid Na (0,66 g, 28,7 mmol) with 1ml of Et_2O. This suspension was stirred under N_2 atmosphere for 3 hours until all Na solid formed NaOMe. Then 40 ml of Et_2O and 3-acetylpyridine (2 ml, 18,2 mmol) is added to NaOMe light grey solution, forming a yellow suspension, which is stirred for 10 minutes. Then, a solution of 2,6-ethyl dipicolinate (1 g, 4,5 mmol) in Et_2O (40 ml) was added dropwise to the yellow suspension. Reflux was maintained for 3,5 hours. The yellow suspension became brown-yellow and then dark green. The dark green solid was filtered and suspended in 60 ml of H_2O and it was added AcOH (4 ml) until having pH=4. This suspension was stirred for 40 minutes, then was filtered and the brown solid obtained was washed with H_2O and Et_2O. The solid is solved in THF (80 ml) it is obtained a

suspension. The suspension was filtered and a brown solid was obtained, which is washed with water and then with Et_2O, obtaining a yellow solid. The mother liquor was carried to dryness in the rotary evaporator, obtaining a pale orange solid. Two solids were characterized by ^1H NMR.

❖ Third Stage: Synthesis of H_2L2

To a suspension of H2LB (0,5 g, 1,3 mmol) in MeOH (100 ml) was added N_2H_4 65% (0,24 ml, 3,2 mmol), the grey suspension turned a yellow solution. This solution was stirred for 5 hours. The half of the solution was refluxed for 2 hours (F2) and then it was fileted obtaining a white solid. The other half of the solution (F1) was filtered, obtaining a white solid. These two white solids were characterized by ^1H NMR.

6.2.3 Synthesis of H_2L3

❖ First Stage: Synthesis of dimethyl 2,5-pyridinedicarboxylate

To a solution of 2,5-pyridinedicarboxylic acid (5,1 g, 30,5 mmol) in MeOH (200 ml) was added dropwise thiolyl chloride (5,4 ml, 74,4 mmol) and was brought to reflux for two hours. The resulting light yellow solution was allowed to cool to room temperature and the solution was carried to dryness in the rotary evaporator. To quench all HCl, 5 extractions of $CHCl_3$ and water were carried out. Then all the $CHCl_3$ was removed in the rotary evaporator. A white solid was obtained with 78% yield. This solid was characterized by ^1H NMR.

❖ Second Stage: Synthesis of dimethyl 5-(methoxycarbonyl)picolinic acid

To a solution of dimethyl 2,5-pyridinedicarboxylate (1g, 5,1 mmol) in MeOH (100 ml) was added potassium hydroxide (0.4g, 7,1 mmol). The reaction was done in a chiller by 3 hours. The suspension is filtered. The solution is carried to dryness in the rotary evaporator. A light yellow solid was obtained with 56% yield. This solid was characterized by ^1H NMR.

6.2.4 Synthesis of H_4L4

- First Stage: Synthesis of H_2LD

First Approach

MeOH (15 ml) is added dropwise and gradually to solid Na (0,33 g, 13,8 mmol) with 1ml of Et_2O. This suspension was stirred under N_2 atmosphere for 3 hours until all Na solid formed NaOMe. Then a solution of 2,6-diacetylpyridine (0,42 g, 2,6 mmol) in Et_2O (30 ml) was added dropwise to NaOMe light grey suspension, forming a yellow suspension, which is stirred for 10 minutes. Then, a solution of dimethyl isophthalate (1 g, 5,1 mmol) in Et_2O (30 ml) was added dropwise to the yellow suspension. Reflux was maintained for 4 hours. The yellow suspension became an orange suspension after the first 60 minutes of reflux. The orange solid was filtered and suspended in 40 ml of H_2O and it was added AcOH (5 ml) until having pH=4. This suspension was stirred for 15 minutes, then was filtered and the brown solid obtained was washed with H_2O and Et_2O. The solid was solved in $CHCl_3$ (30 ml) and H2O (30 ml), a suspension was obtained. The suspension was filtered and a brown solid was obtained, which was not soluble in any solvent. The mother liquor was extracted with a saturated solution of NaCl until having pH=5. A brown solid was obtained by using the rotary evaporator, and was characterized by ^1H NMR.

Second Approach

A solution of dimethyl isophthalate (1 g, 5,2 mmol) in Et_2O (100 ml) is stirred under nitrogen atmosphere. NaH dispersion in mineral oil was suspended in hexane to remove this mineral oil, and then a solution of 2,6-diacetylpyridine (0,42 g, 2,6 mmol) in Et_2O (10 ml) is added to the pure NaH, obtaining a grey suspension. This 2,6-diacetylpyridine with NaH in Et_2O grey suspension is added dropwise into the dimethyl isophthalate solution. A grey suspension is obtained. Stirring was maintained for 1 hour (room temperature) and the reaction is monitored by TLC. Reflux is maintained for 2 hours and 50 minutes, and a light yellow suspension is obtained. The resulting suspension quenched with EtOH (2 ml), until the absence of H_2 apparition. This suspension is carried to dryness in the rotary evaporator. A few drops of HCl 1,22 M solution are added to red solid suspended in H_2O (100 ml) until pH=4, then the suspension is stirred for 10 minutes. This suspension is filtered and a grey solid is obtained. This solid is washed with H_2O, Et_2O and $CHCl_3$. When this solid is washed in Et_2O a part of it is solubilized and this solid obtained by carrying Et_2O to dryness is collected. The rest of the solid, insoluble in Et_2O and washed with $CHCl_3$ is boiled in acetone and this warm solution is filtered. This acetone is carried to dryness and a brown shiny solid is obtained. This solid is solved in $CHCl_3$ a part of it is soluble in $CHCl_3$.

This suspension is filtered, a white solid is obtained. The resultant $CHCl_3$ solution is carried to dryness and a brown solid is obtained. These solids were characterized by ^1H NMR.

6.3 SYNTHESIS OF COMPLEXES

The synthesis of the mononuclear complex of Fe(II) is based in this general procedure:

$$\mathbf{2\ H_2L1 + Fe(II)\ salt \rightarrow [Fe(H_2L1)_2]^{2+}}$$

A solution/suspension of the H_2L1 ligand in a solvent was added dropwise into a Fe(II) salt and ascorbic acid (~1mg) solution in the same or different solvent, under soft stirring or without stirring. The mixtures which were stirred, were stirred for 30-60 minutes at room temperature. In the case of obtaining a solution, it was filtered and layered in different types of antisolvent. In the case of obtaining a suspension, it was filtered, the solid was collected, characterized by IR spectroscopy resolved and layered in different antisolvents. Instead using ascorbic acid, many reactions had been realized in the glove box by doing the same procedure.

10. CONCLUSIONS

In order to achieve new Fe(II) complexes featuring spin CrossOver properties, a new research project has been carried out from scratch. New ligands which promote SCO behaviour have been synthesized. Given the novelty of these ligands, some syntheses have not been as expected, nevertheless, a new alternative ones have been proposed. Due to the interesting properties that this complexes could exhibit, these new alternative synthesis routes make possible the continuation of this project.

Concerning to the Fe(II) complexes synthesized, it is important to obtain crystals and to find suitable crystallization conditions is necessary, also long periods are required for the complexes to crystallize in single crystal structure (at least 3-6 weeks). Regarding to the organic ligands synthesized, the presence of pyridinic nitrogen atoms in the extreme of the ligands essentially increases the possibility of a retro-Claisen cleavage. For this reason it has been obtained an unexpected Fe(II) complex which doesn't exhibit SCO properties, since the Fe(II) metal is coordinated to an oxygen instead of a nitrogen due to the cleavage of the ligand through a retro-Claisen.

The new ligands designed, synthesized and characterized and the new alternative syntheses proposed during this project represent a starting point for the development of new promising materials which could present fascinating applications.

11. REFERENCES AND NOTES

1. Pelter, M. W.; McQuade, J. Brewing Science in the Chemistry Laboratory: A "Mashing" Investigation of Starch and Carbohydrates. *J. Chem. Educ.* **2005,** *82,* 1811-1812.
2. (a) Evans, D. A.; Fitch, D. M.; Smith, T. E.; Cee, V. J. Application of Complex Aldol Reactions to the Total Synthesis of Phorboxazole B. *J. Am. Chem. Soc.* **2000,** *122*, 10033-10046; (b) Jenkins, T.; Mott, L. Ion Exchange Resins Used in Nuclear Waste Disposal. *Environ. Sci. Technol.* **1999**, *86*, 122-134; (c) Mastronardi, F.; Gutmann, B. Kappe, O. Continuous Flow Generation and Reactions of Anhydrous Diazomethane Using a Teflon AF-2400 Tube-in-Tube Reactor. *Org. Lett.* **2013**, *15*, 5590-5593; (d) Mawhinney, R. C.; Muchall, H. M.; Peslherbe, G.H. A Computational Study of the 1,3-Dipolar Cycloaddition Reaction Mechanism for Nitrilimines. *Can. J. Chem.* **2005**, *35*, 1615-1625.
3. Peacock-Lopez, E. Exact Solutions of the Quantum Double Square-Well Potential. *Chem. Ed.* [Online] **2007,** *11*, 383-393 http://chemeducator.org/bibs/0011006/11060380lb.htm (accessed Aug 23, 2007).
4. Wilkins, T. D.; Tucker, K. D. Detection, Isolation, and Purification of Clostridium Difficile Toxin A with Toxin Receptors. U.S. Patent 5,098,826, March 24, 1992.
5. Chang, R. *General Chemistry: The Essential Concepts,* 3rd ed.; McGraw-Hill: Boston, 2003.
6. Gbalint-Kurti, G. G. Wavepacket Theory of Photodissociation and Reactive Scattering. In *Advances in Chemical Physics;* Rice, S. A., Ed.; Wiley: New York, 2004; Vol. 128; p 257.
7. Omega-3 Fatty Acids: Chemistry, Nutrition, and Health Effects; Shahidi, F., Finley, J. W., Eds.; ACS Symposium Series 788; American Chemical Society: Washington, DC, 2001.
8. Powder Metallurgy. Kirk-Othmer Encyclopedia of Chemical Technology, 3rd ed.; Wiley: New York, 1982; Vol. 19, pp 28-62.
9. Gehring, A. PhD. Dissertation, Harvard University, 1998.
10 Winstein, S. In *University Chemical Education,* Proceedings of the International Symposium on University Chemical Education, Frascati (Rome), Italy, October 16-19, 1969; Chisman, D. G.. Ed.; Butterworths: London, 1970.
11. National Library of Medicine. Environmental Health and Toxicology: Specialized Information Services. http://sis.nlm.nih.gov/enviro.html (accessed Aug 23, 2004).

APPENDICES

APPENDIX 1: NMR OF LIGANDS

1. *^{1}H-NMR of H_2LB first approach*

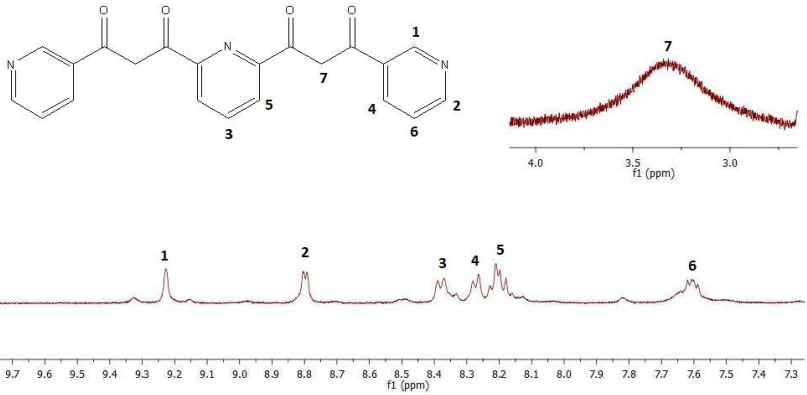

2. *^{1}H-NMR of H_2LB second approach*

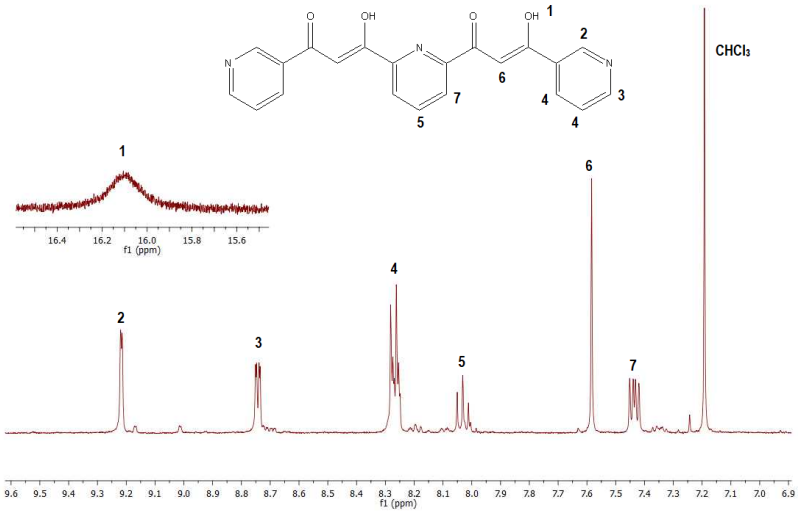

3. *^{1}H-NMR of H_2L2*

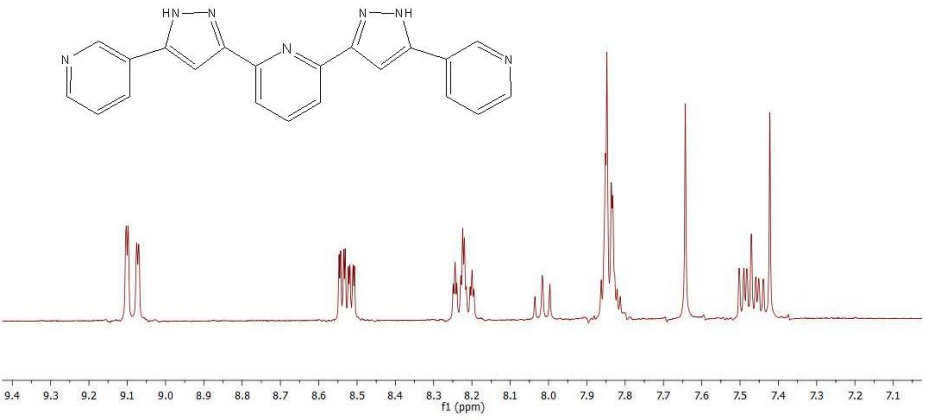

4. *^{1}H-NMR of H_2L2 dimethyl* 5-(methoxycarbonyl)picolinic acid

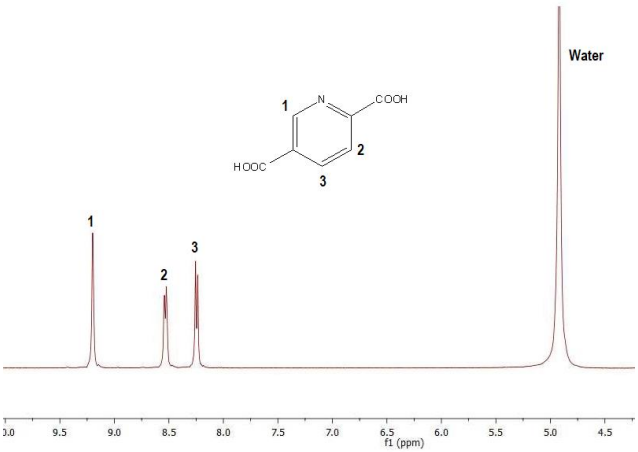

5. *^{1}H-NMR of H_2LD first approach*

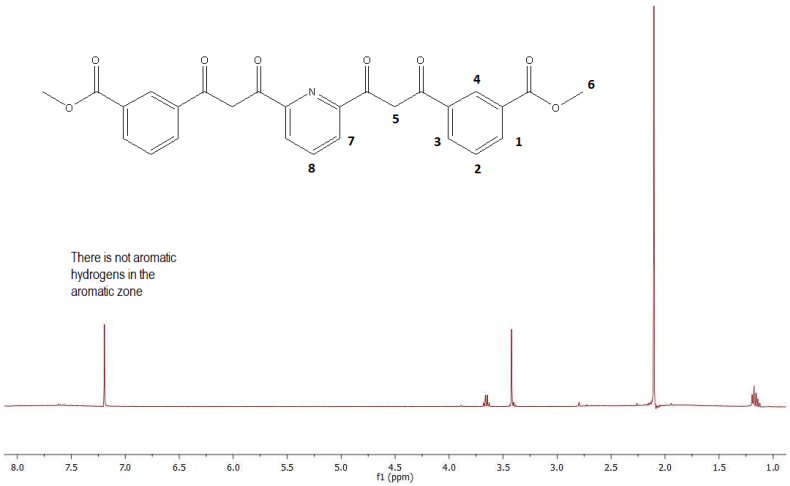

6. *^{1}H-NMR of H_2LD second approach*